RESEARCH

The relevance of tumor target expression levels on IgA-mediated cytotoxicity in cancer immunotherapy

Chilam Chan[1] · Núria Casalé Cabanes[1] · J. H. Marco Jansen[1] · Joël Guillaume[1] · Maaike Nederend[1] · Elsemieke M. Passchier[1] · Valentina E. Gómez-Mellado[2] · Matthias Peipp[3] · Marianne Boes[1,4] · Geert van Tetering[1] · Jeanette H. W. Leusen[1]

Abstract

Recent advances in cancer immunotherapy, particularly the success of immune checkpoint inhibitors, have reignited interest in targeted monoclonal antibodies for immunotherapy. Antibody therapies aim to minimize on-target, off-tumor toxicity by targeting antigens overexpressed on tumor cells but not on healthy cells. Despite considerable efforts, some therapeutic antibodies have been linked to dose-limiting side effects. Our hypothesis suggests that the efficacy of IgG leads to a lower target expression threshold for tumor cell killing, contributing to these side effects. Earlier, therapeutic IgG antibodies were reformatted into the IgA isotype. Unlike IgG, which primarily engages Fc gamma receptors (FcγR) to induce antibody-dependent cellular cytotoxicity (ADCC) by NK cells and antibody-dependent cellular phagocytosis (ADCP) by monocytes/macrophages, IgA antibodies activate neutrophils through the Fc alpha receptor I (CD89, FcαRI). In previous studies, it appeared that IgA may require a higher target expression threshold for effective killing, and we aimed to investigate this in our current study. Moreover, we investigated how blocking the myeloid checkpoint CD47/SIRPα axis affect the target expression threshold. Using a tetracycline-inducible expression system, we regulated target expression in different cell lines. Our findings from ADCC assays indicate that IgA-mediated PMN ADCC requires a higher antigen expression level than IgG-mediated PBMC ADCC. Furthermore, blocking CD47 enhanced IgA-mediated ADCC, lowering the antigen threshold. Validated in two in vivo models, our results show that IgA significantly reduces tumor growth in high-antigen-expressing tumors without affecting low-antigen-expressing healthy tissues. This suggests IgA-based immunotherapy could potentially minimize on-target, off-tumor side effects, improving treatment efficacy and patient safety.

Keywords Antigen expression levels · CD47/SIRPα · IgA · Immunotherapy · Neutrophils

Abbreviations

ADCC	Antigen-dependent cell cytotoxicity
ADCP	Antibody-dependent cell phagocytosis
ATCC	American Type Culture Collection
BLI	Bioluminescence imaging
CDC	Complement-dependent cytotoxicity
Dox	Doxycycline
EGFR	Epithelial growth factor receptor
E:T	Effector to target ratio
FCS	Fetal calf serum
FcαRI	Fc alpha receptor I
FcγRs	Fc gamma receptors
HER2	Human epithelial receptor 2
IHC	Immunohistochemistry staining
i.p.	Intraperitoneally
i.v.	Intravenously
mAbs	Monoclonal antibodies

Geert van Tetering and Jeanette H. W. Leusen have contributed equally to this work.

✉ Jeanette H. W. Leusen
   J.H.W.Leusen@umcutrecht.nl

1   Center for Translational Immunology, University Medical Center, Heidelberglaan 100, 3584 CX Utrecht, The Netherlands

2   Center for Molecular Medicine, University Medical Center Utrecht, Utrecht, The Netherlands

3   Division of Antibody-Based Immunotherapy, Department of Medicine II, Christian Albrechts University Kiel and University Medical Center Schleswig-Holstein, Campus Kiel, 24105 Kiel, Germany

4   Pediatrics Department, University Medical Center, Utrecht, The Netherlands

🍊 Springer

PMN   Human polymorphonuclear leukocytes
PBMC   Peripheral blood mononuclear cells
RBC   Red blood cell
RPMI   Roswell Park Memorial Institute
rtTA   Reverse transcriptional activator
s.c.   Subcutaneous
TAA   Targeting tumor-associated antigens

Introduction

Immunotherapy using IgG monoclonal antibodies (mAbs) and immune checkpoint inhibitors has emerged as an important approach in the current cancer treatment regimen. The mechanisms of action of IgG antibodies include Fab-mediated, Fc-mediated, or a combination of both interactions. For instance, through Fab-mediated binding, antibodies can effectively disrupt the interaction between the receptor and its natural ligand, resulting in the impairment of downstream signaling pathways [1, 2]. Moreover, IgG antibodies can activate various Fc-mediated effector functions including the initiation of the complement-dependent cytotoxicity (CDC) pathway through engagement with the C1q binding site. Additionally, IgG antibodies can activate immune responses by engaging with Fc gamma receptors (FcγRs), thereby inducing ADCC and ADCP [3–5].

NK cell-mediated ADCC involves the release of granzymes and perforins, and is induced by the interaction between the antibody's Fc domain and FcγRIIIa, important for tumor cell elimination [4, 6–8]. Alternatively, neutrophils are another immune cell subset capable of inducing ADCC, through engagement of another FcγR, namely FcγRIIA [9]. However, neutrophils also express an inhibitory receptor, FcγRIIB, and a non-signaling receptor, FcγRIIIB. These two receptors outcompete IgG binding to FcγRIIA and, consequently, neutrophil-mediated ADCC is not efficiently induced by IgG. As a result, ADCC and ADCP by myeloid cells are predominantly dependent on monocytes/macrophages rather than neutrophils [9].

Despite the promising therapeutic benefits of IgG mAbs, side effects are common. These side effects can be severe, necessitating treatment modification or discontinuation, negatively impacting patients' quality of life [10, 11]. Side effects caused by targeting tumor-associated antigens (TAAs) expressed on healthy tissues, known as on-target, off-tumor side effects, are especially concerning. These have been observed with commonly used monoclonal antibodies such as cetuximab, trastuzumab and rituximab. Cetuximab, an anti-epithelial growth factor receptor (EGFR) antibody, has been linked to skin toxicity, resulting in mild to severe rashes and eczema symptoms, due to EGFR expression on keratinocytes [11–14]. Whereas trastuzumab, an antibody directed against the human epithelial receptor 2 (HER2), is often used in the treatment of HER2-positive breast cancer patients. However, treatment has been associated with cardiotoxicity, which has been linked to HER2 expression in cardiomyocytes [15–17]. Cardiotoxic effects have been observed when trastuzumab was combined with chemotherapeutic agents known to cause cardiac stress. Additionally, patients with pre-existing cardiac conditions are more vulnerable to trastuzumab-induced cardiotoxicity, making it an unsuitable treatment approach for this patient population [18]. In the context of hematological tumors, Rituximab, used in the treatment of non-Hodgkin's lymphoma, has been shown to deplete healthy B cells. This poses a concern for some pediatric and adult patients, as it can occasionally lead to immunoglobulin insufficiency, making them more susceptible to infections [19, 20].

TAAs are generally characterized by higher expression levels on tumor cells compared to healthy tissues [21]. Others have demonstrated attempts to precisely target high antigen expression levels, with success in avoiding side effects associated with unintentional targeting of healthy tissue [22]. For example, there have been no reports of skin toxicity from nimotuzumab, an EGFR antibody that selectively binds bivalently, thus only cells with high EGFR expression levels [23]. Hence, a viable approach to mitigate on-target, off-tumor side effects is to direct antibodies toward cells with high antigen expression levels. Existing literature suggests that there is a threshold for IgG-mediated targeting [24], and this threshold is relatively low, possibly failing to distinguish between tumor cells with high antigen expression and healthy cells with low antigen expression [25–27]. In contrast, antibodies of a different isotype, IgA antibodies, were reported to require higher expression levels to efficiently kill the target cell [26, 28], suggesting that IgA are less likely to cause on-target, off-tumor side effects.

Therapeutic IgA antibodies have recently been explored as an alternative to conventional IgG-based immunotherapies [29–32]. IgA antibodies have demonstrated comparable Fab-binding characteristics as their IgG counterparts. Moreover, IgA can activate Fc-dependent effector functions, such as ADCC and ADCP, albeit by interacting with other immune cells and Fc receptors [28, 33–35]. The primary receptor for IgA is FcαRI (CD89), which is predominantly expressed on neutrophils, eosinophils, monocytes, and macrophages [36, 37]. As previously mentioned, neutrophils are not efficiently activated by IgG antibodies. In comparison, IgA binding to FcαRI robustly induces neutrophil-mediated ADCC against tumor cells [28, 38–40]. IgA therapy as cancer therapy holds promise as a strategy to reduce on-target, off-tumor side effects.

IgA predominantly activates neutrophils as the primary subset of effector cells, yet their activity is also regulated by myeloid checkpoints, among other regulatory mechanisms. To avoid immune surveillance, tumor

cells overexpress myeloid checkpoint molecules. The CD47/SIRPα axis is one of such interactions between tumor cells and neutrophils [9, 41–44]. Combining IgA immunotherapy with CD47 blockade has been shown to improve IgA-mediated neutrophil cytotoxicity [31, 45, 46]. However, the effect of the CD47/SIRPα axis on the antigen expression threshold required for effective IgA therapy has yet to be investigated.

We hypothesized that IgA may require higher antigen expression levels than IgG for the induction of effective ADCC, and may potentially be influenced by the myeloid checkpoint axis CD47/SIRPα. To address this possibility, we used doxycycline-inducible cell lines expressing HER2 or EpCAM to investigate how antigen expression levels influence ADCC mediated by both IgG and IgA antibodies. In addition, we assessed the role of the CD47/SIRPα axis in IgA-induced neutrophil cytotoxicity.

Materials and methods

Antibodies

Trastuzumab (Herceptin, an anti-HER2 IgG1 antibody) was purchased from the University Utrecht pharmacy. IgA3.0 trastuzumab was generated by Wuxi Biologics through the expression in CHO-K1 cells, followed by affinity purification. The CD47 blocking protein (SIRPα fusion protein) was created as an engineered human SIRPα D1 domain fused to IgG1 L234A/L235A/P329G (LALAPG), demonstrating high affinity for both mouse and human CD47, as previously described [47]. The SIRPα fusion protein, IgG1 human engineered ING-1 (heING1, anti-EpCAM), IgA3.0 heING1 and mCD20 abs were all produced and affinity purified in-house using the previously described method [48]. In brief, antibodies were produced via transient transfection of ExpiCHO-S cells (Thermo Fisher Scientific). Subsequently, the antibody-containing supernatant was subjected to affinity chromatography. IgG antibodies were purified using a HiTrap® Protein A column (Cytiva) connected to an ÄKTA liquid chromatography system (Cytiva); whereas, IgA3.0 antibodies were purified using a HiTrap® KappaSelect column (Cytiva). The IgA3.0 eluate was further purified using size exclusion chromatography; whereas, the IgG eluate was dialyzed against PBS overnight. Purified antibodies were filtered through a 0.22 μm filter, and their concentrations were determined by measuring UV absorbance at 280 nm, using the corresponding extinction coefficient (ε280). Hereafter, all IgA antibodies are of the IgA3.0 isotype unless stated otherwise.

Cell culture

Cell lines were obtained from American Type Culture Collection (ATCC) and cultured at 37 °C in a humidified incubator containing 5% CO_2 unless stated otherwise. SK-BR-3, BCL-1, A431-luc2 and A431-luc2-HER2 cells were cultured in Roswell Park Memorial Institute (RPMI, Thermo Fisher Scientific) supplemented with 10% heat-inactivated fetal calf serum (FCS) and 100 U/mL penicillin–streptomycin (Pen/Strep, Gibco, life technologies), hereafter called complete RPMI medium. A431-luc2 cells were generated by lentiviral transduction with a luciferase-GFP construct, and A431-luc2-HER2 was additionally retrovirally transduced with HER2. A431-luc2-HER2 cells were cultured with complete RPMI medium under 0.5 μg/mL puromycin (Sigma) selection. MDA-MB-175, MDA-MB-453 and MDA-MB-468 were cultured in Leibovitz's L-15 (Thermo Fisher Scientific) supplemented with 10% FCS and 100 U/mL Pen/Strep without CO_2 exchange. Cells were not cultured beyond 20 passages and were regularly tested for mycoplasma contamination using a Mycoalert mycoplasma detection kit (Lonza).

Generation of tetracycline (Tet) inducible cell lines

Tet-inducible cell lines were generated by lentiviral transduction, using the pINDUCER20 plasmid kindly gifted by Hugo Snippert. The plasmid containing either HER2 or EpCAM genes was introduced into HEK293T and HeLa cells, respectively. The pINDUCER20 plasmid incorporates the target gene under the regulation of a doxycycline (dox)-inducible promoter based on the bacterial Tet-on system. This system enables gene expression upon exposure to dox in a concentration-dependent manner. Subsequently, cells were sorted and subcloned to establish stable cell lines with consistent and homogenous induction profiles. Clones were screened by inducing cells for 24-h with titrated dox concentrations, and induction was confirmed through flow cytometry analysis. HeLa cells with inducible EpCAM expression (HeLa-EpCAM) and HEK293T cells with inducible HER2 expression (HEK293T-HER2) were cultured in RPMI (Thermo Fisher Scientific) supplemented with 10% Tet System Approved FBS (Takara), 100 U/mL Pen/Strep, and 0.3 μg/mL or 0.75 μg/mL puromycin, respectively. MDA-MB-231 cells with inducible HER2 expression (MDA-MB-231-HER2) were maintained in RPMI (Thermo Fisher Scientific) supplemented with 10% Tet System Approved FBS (Takara) and 100 U/mL Pen/Strep.

Flow cytometry

Surface protein expression was analyzed with flow cytometry. A total of 1×10^5 cells were stained with antibody (Table 1) in FACS buffer (PBS, 0.01% bovine serum

Table 1 Antibodies for flow cytometry

Target	Fluorophore	Clone	Manufacturer
CD47	Pacific blue	CC2C6	Biolegend, 323,127
CD47	Unconjugated	CC2C6	Biolegend, 323,102
HER2	Alexa fluor 647	24D2	Biolegend, 324,412
HER2	Unconjugated	H2Mab-77	Biolegend, 399,402
EpCAM	PE	9C4	Biolegend, 324,205
EpCAM	Unconjugated	9C4	Biolegend, 324,201
mCD20	APC	SA275A11	Biolegend, 150,411

albumin, 0.01% sodium azide) for 45 min on ice. To determine the absolute molecules per cell we performed a QIFIKIT (Agilent/Dako) analysis. Assay was performed according to manufacturer's instructions. Cells were stained with a saturating concentration of 10 ug/mL unconjugated mouse IgG monoclonal antibody directed against HER2 or EpCAM (Table 1) Measurements were performed on BD FACS Canto II.

ADCC assays

[51]Cr release ADCC assays were carried out as previously described [49]. When applicable, the expression of the target antigen was induced in Tet-inducible cell lines one day prior to the ADCC assay. To induce target antigen expression, cells were treated with doxycycline at concentrations of 0–1 µg/mL in a three-fold dilution series, and incubated for 24-h. Target cells were labeled with 100 µCi chromium-51 (PerkinElmer) per million cells for at least 2 h at 37 °C and 5% CO_2. After labeling, the cells were washed three times with medium. For certain experiments, cells were either pretreated with 10 µg/mL of SIRPα fusion protein for 30 min at room temperature, or the SIRPα fusion protein was directly added to the co-culture at a final concentration of 10 µg/mL, aiming to block CD47. Human polymorphonuclear leukocytes (PMNs) and peripheral blood mononuclear cells (PBMCs) were isolated from peripheral blood from healthy donors at the UMC Utrecht using Ficoll density gradient centrifugation. After collecting the PBMC layer, the remaining pellet was subjected to erythrocyte lysis using red blood cell (RBC) Lysis Buffer (Biolegend) and PMNs were collected. PMNs and PBMCs were then co-cultured with the labeled target cells at effector-to-target (E:T) ratios of 40:1 and 100:1, respectively. Antibodies were added at the specified concentrations for each experiment. After a 4-h incubation at 37 °C and 5% CO_2, plates were centrifuged, and the supernatant was transferred to a lumaplate (PerkinElmer) for measurement on a beta-gamma counter to quantify radioactive scintillation (in cpm) (PerkinElmer). Specific lysis was calculated using the formula: ((Experimental cpm−basal cpm)/(maximal cpm−basal cpm))×100. Maximal cpm was determined by treating target cells with 5% Triton X-100 (Sigma-Aldrich); while, basal cpm was determined by chromium release of target cells in the absence of antibodies and effector cells.

Mice

All mice were bred and maintained at Janvier Labs in Paris, France. After being transported to University of Utrecht's Central Laboratory Animal Research Facility for the experiment, mice were acclimatized for at least one week prior to the start of the experiment. Mice were housed in a temperature-controlled environment with a 12:12 h light–dark cycle with access to food and water ad libitum.

A431 long i.p. xenograft model

Female human FcαRI (CD89) transgenic (Tg) mice were used in the experiment, which were previously generated at UMC Utrecht and backcrossed on a SCID (CB-17/Icr-Prkdcscid/scid/Rj) background [50]. Female transgene-negative (non-Tg) littermates were used in both the solvent control (PBS) and the IgG treatment groups. Because these treatment groups do not receive IgA, the presence of CD89 is not required. Importantly, there are no differences in tumor outgrowth between CD89 Tg mice and non-Tg littermates, allowing for combined use in the same experiment [51]. All mice ranged in age from 8 to 26 weeks at the time of the experiment. Both the treatment and the analysis were double-blind.

For the A431-luc2 model, a total of 1×10^5 A431-luc2 cells were injected intraperitoneally (i.p.) on day 0. On days 3 and 7, PEG-G-CSF (20 g) was subcutaneously (s.c.) injected. The tumors were measured using bioluminescence imaging (BLI) after 4 days, and the treatment groups were randomized based on tumor size, with treatment beginning on day 5. Mice were treated i.p. with either 2 mg/kg IgG HER2 (trastuzumab) once per week or 2 mg/kg IgA HER2 three times per week till the end of the experiment. Because IgA has a shorter half-life than IgG, it was administered more frequently to match IgG serum levels [52]. Additionally, CD47 was blocked in combination with IgA treatment. On day 5, 14, 24 and 33, an amount of 30 mg/kg SIRPα fusion protein was injected intraperitoneally. As a solvent control, mice received PBS. A total of 10 mice were used for each treatment group. Tumor growth was monitored twice a week using BLI. Mice were sacrificed by cervical dislocation upon reaching humane endpoint.

For the A431-luc2-HER2 model, 1×10^5 A431-luc2-HER2 cells were injected i.p. on day 0. On day 6, 20 µg of PEG-G-CSF was administered s.c., followed by a BLI measurement. Subsequently, treatment groups were randomized based on tumor size, and treatment (i.p.) started on day 7.

IgG HER2 received 10 μg on days 7 and 14; while, IgA HER2 received 10 μg daily for 10 days. The vehicle control group received PBS on days 7 and 14. BLI measurements were performed twice a week to monitor tumor outgrowth. Mice were euthanized by cervical dislocation upon reaching the humane endpoint.

mCD20 B cell depletion assay

CD89 Tg mice backcrossed on a Balb/c background were given a single intravenous (i.v.) injection of either PBS, 5 mg/kg murine IgG2a ADCC + mCD20 (modified mouse IgG with enhanced ADCC capacity (afucosylated) [53]) or IgA-Alb8 mCD20 (with improved half-life, patent US20170210789A1). 9 mice were included per group. B cell depletion was determined at different time points in blood, liver, spleen, lymph nodes and bone marrow by flow cytometry analysis (Supplementary Table 1).

BCL-1 i.v. syngeneic mouse model

A BCL-1 lymphoma mouse model was established using female CD89 Tg Balb/c mice. On day 0, 5×10^5 BCL-1-luc2 cells were injected i.v. along with a dose of PEG-G-CSF (20 ug, s.c.). On day 7, another dose of PEG-G-CSF was administered. Treatment with PBS, 6 mg/kg IgG2a ADCC + mCD20 or 6 mg/kg IgA-Alb8 mCD20 started at day 3. IgA was given on days 3,5,7,10,12 and 14; while, IgG was given on days 3 and 10. The dosing regimen for each antibody was adjusted to ensure similar serum levels [48]. BLI was performed twice a week to monitor tumor growth. Both the treatment and the analysis were double-blind. Mice were sacrificed by cervical dislocation upon reaching humane endpoint.

Ethical approval

This study involves human participants and was approved by UMC Utrecht 07–125. Participants gave informed consent to participate in the study before taking part. All animal experiments followed international guidelines and were approved by the national Central Authority for Scientific Procedures on Animals (CCD) and the local experimental animal welfare organization (AVD115002016410).

Data processing and statistical analyses

Flow cytometry data were analyzed using FlowJo software (TreeStar). Statistical analyses were performed using GraphPad Prism 9.3.0 (GraphPad Software Inc.). Specific statistical tests performed for each experiment are indicated in the corresponding figure legends. Data are presented as mean ± standard deviation (SD) or standard error of mean (SEM) and a p value of less than 0.05 was considered statistically significant. Graphs and figures were generated using the software, Adobe Illustrator and Biorender. Imaging data were analyzed using Imaris (Bitplane).

Data availability

The data generated in this study are available upon request from the corresponding author.

Results

HER2 expression levels influence IgG and IgA-mediated ADCC capacity in breast cancer cell lines.

HER2 expression levels are important in determining the course of immunotherapy treatment for breast cancer patients. The HER2 classification of breast tumors is determined through immunohistochemistry staining (IHC), which uses a scale ranging from 0 to 3 + . Only a score of 3 + is considered HER2-positive, leading to treatment with trastuzumab (hereafter IgG HER2). We selected four cell lines, each of which corresponded to one of the four HER2 scores. Specifically, SK-BR-3 (3 +) is classified as HER2-positive; while, MDA-MB-453 (2 +) expresses lower HER2 levels, falling within the borderline positive range. MDA-MB-175 (1 +) and MDA-MB-468 (0 +) are both categorized as HER2-negative.

We translated these IHC scores into absolute numbers of molecules expressed on the cell surface per cell using QIFIKIT analysis (Error! Reference source not found.**A).** Subsequently, we investigated how these expression levels correlated with the ADCC capacity elicited by IgG HER2 and IgA HER2 antibodies. All four cell lines were tested in a 4-h ^{51}Cr release assay using PBMCs as effector cells to induce IgG-mediated killing and PMNs for IgA-mediated killing (Fig. 1B). In a previous study, we tested the ADCC capacity of IgG using PMNs and IgA using PBMCs [49]. However, we observed no to limited killing under these conditions. Therefore, in this study we tested IgA with PMNs and IgG with PBMCs to better reflect the primary effector mechanisms of each isotype. As expected, both HER2-negative cell lines, MDA-MB-468 (0) and MDA-MB-175 (1 +), remained resistant to killing. Moreover, both IgG HER2 and IgA HER2 induced killing of SK-BR-3 (3 +) cells. Additionally, we observed comparable lysis with IgG HER2 against SK-BR-3 (3 +) and MDA-MB-453 (2 +) at 10 μg/mL. In contrast, IgA HER2 did not significantly induce any killing against MDA-MB-453, suggesting that the IgA-induced ADCC capacity is less efficient at lower expression levels (Fig. 1A, B).
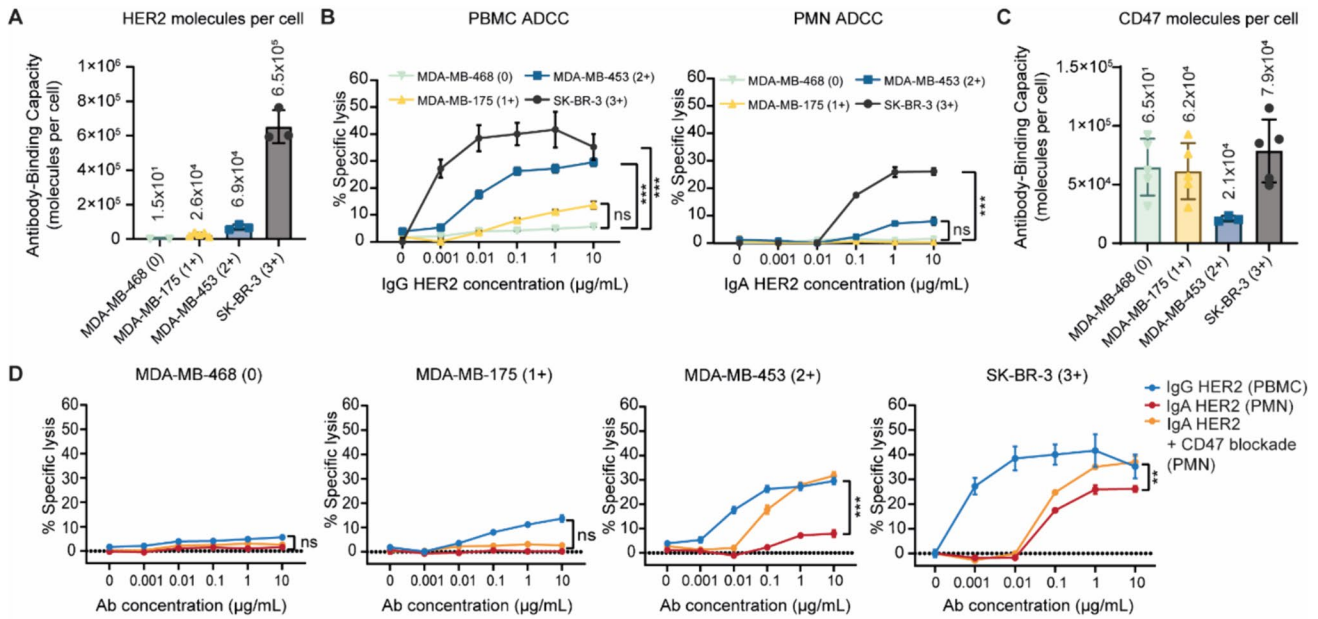
Fig. 1 Influence of HER2 and CD47 expression levels on IgG and IgA-mediated ADCC capacity in breast cancer cell lines. **A** HER2 expression levels depicted as number of molecules per cell on breast cancer cell lines: MDA-MB-468, MDA-MB-175, MDA-MB-453, and SK-BR-3. Expression levels were quantified by QIFIKIT using 10 μg/mL mIgG1 anti-human HER2 antibody. Data shown as mean ± SD from three independent experiments. **B** PBMC- and PMN-mediated ADCC of the breast cancer cell lines, using IgG1 HER2 and IgA HER2, respectively. Significance was determined as compared to MDA-MB-468. Assay was performed in technical triplicates and repeated independently with three donors. Specific lysis is shown as mean ± SEM for one representative experiment. ns > 0.05, ***p < 0.001, by two-way ANOVA followed by Tukey's multiple comparisons test. **C** CD47 expression levels depicted as number of molecules per cell on MDA-MB-468, MDA-MB-175, MDA-MB-453, and SK-BR-3. Expression levels were quantified by QIFIKIT using 10 μg/mL mIgG1 anti-human CD47 antibody. Data shown as mean ± SD from three independent experiments. **D** ADCC assay against breast cancer cell lines mediated by IgG1 HER2, IgA HER2 and IgA HER2 in combination with CD47 blockade. CD47 was pre-blocked using SIRPα fusion protein at 10 μg/mL. In all ADCC assays, PBMCs were used as effector cells in IgG ADCCs (E:T ratio 100:1); while, PMNs (E:T ratio 40:1) were used for IgA ADCCs. Antibody concentrations ranged between 0 and 10 μg/mL. Assay was performed in technical replicates (n = 3) and repeated with three independent donors in separate assays. Specific lysis is shown as mean ± SEM for one representative experiment from one donor. ns > 0.05, **p < 0.01, ***p < 0.001, by two-way ANOVA followed by Tukey's multiple comparisons test

Blocking the CD47/SIRPα axis enhances IgA-mediated ADCC capacity in breast cancer cell lines

Checkpoint molecules are often overexpressed on tumor cells as a mechanism to hamper immune responses against the tumor and thus avoid immune surveillance. The CD47/SIRPα axis is one of such checkpoints that affects myeloid cells and, as a result impair PMN-mediated lysis by IgA antibodies. We investigated whether CD47 expression could account for the observed difference between IgG and IgA against MDA-MB-453. We quantified the CD47 expression levels on our panel of breast cancer cell lines using QIFIKIT analysis. Surprisingly, MDA-MB-453 expressed lower CD47 levels when compared to the other cell lines (Fig. 1C). Despite the lower CD47 expression level, CD47 blockade improved IgA-mediated lysis by PMNs to lysis levels comparable to IgG PBMC-mediated ADCC (Fig. 1D). Moreover, combining IgA HER2 and CD47 blockade improved ADCC against SK-BR-3, though the improvement was less considerable than when MDA-MB-453 was targeted. The combination of IgG HER2 and CD47 blockade showed no significant differences when compared to IgG HER2 alone (Supplemental Fig. 1), most likely due to the lack of SIRPα expression on the NK cells, the main effector cell population in the PBMC fraction used in this assay. IgG not only induced ADCC at lower expression levels, but is also more effective at lower antibody concentrations. Furthermore, the combination strategy was ineffective in inducing killing of the two HER2-negative cell lines, MDA-MB-468 and MDA-MB-175 (Fig. 1D). This observation supports the notion that CD47 blockade can only improve IgA-mediated killing when a lower limit of antigen is available for IgA targeting to be effective.

Dox-inducible HEK293T-HER2 cells to assess antibody-mediated cytotoxicity.

While previous data indicate that cell surface expression levels can indeed impact antibody-mediated cytotoxicity, it remains difficult to draw solid conclusions due to the inherent phenotypic differences between breast cancer cell lines. To avoid these phenotypical variations, we used a tetracycline-inducible system that allowed us to precisely control antigen expression levels on the cell surface of a single cell line. We introduced HER2 into HEK293T cells under the control of a Tet-On inducible promoter to examine the effect of HER2 expression levels on antibody-mediated cytotoxicity. In the presence of doxycycline (dox), the reverse transcriptional activator (rtTA) binds to the promoter, allowing HER2 transcription (Fig. 2A).

We tested dox concentrations ranging from 0 to 27 μg/mL and incubation times of 18 and 24-h, whereafter the induced HER2 expression was measured by flow cytometry (Supplementary Fig. 2A and B). The HER2 expression level peaked at 1 ug/mL doxycycline. Importantly, we observed a decrease in cell viability above this concentration (data not shown). Moreover, a 24-h incubation period resulted in the utmost induction of HER2 expression. As a result, we proceeded with experiments using a dox concentration range of 0 to 1 ug/mL and a 24-h incubation period. Induced HER2 expression was quantified using QIFIKIT and the expression levels were correlated with the antibody-mediated cytotoxicity measured in a ^{51}Cr release ADCC assay (Fig. 2B).

Following transduction, two clones were selected: HEK293T-HER2-Low, with minimal basal expression and a maximum induction of 1×10^5 HER2 molecules per cell, and HEK293T-HER2-High, with HER2 expression levels ranging from 2 to 5×10^5 HER2 molecules per cell (Fig. 2C). IgG HER2 induced PBMC-mediated killing of HEK293T-HER2-Low cells at a HER2 expression level of 9.5×10^3, peaking at around 20% lysis when the HER2 molecules per cell reached approximately 7.6×10^4 (Fig. 2C). Contrary, IgA HER2 induced PMN-mediated killing in HEK293T-HER2-Low cells, but only achieved a modest 10% lysis. Interestingly, increasing the antigen expression level (HEK293T-HER2-High) had no effect of IgG-mediated killing. However, once the HER2 molecules per cell exceeded 2.1×10^5, IgA-induced killing increased rapidly, reaching lysis of around 20%, which was comparable to IgG-mediated killing. These results suggest that IgA antibodies might require a higher level of antigen expression to efficiently induce ADCC.

The antigen level threshold of IgA is influenced by the CD47-SIRPα axis.

To validate these findings, we introduced HER2 expression into another cell line, MDA-MB-231. We isolated two clones, MDA-MB-231-HER2-Low with inducible HER2 expression levels ranging from negligible to 3.2×10^5 molecules per cell and MDA-MB-231-HER2-High with levels ranging from 4×10^3 to 6.7×10^5 molecules per cell (Fig. 2D).

Remarkably, at the lowest HER2 expression level (2.8×10^4), IgG induced a PBMC-mediated lysis of 30%, which remained constant as HER2 expression levels increased. In contrast, IgA-mediated PMN lysis only occurred at HER2 expression levels exceeding 3×10^5 molecules per cell, and it only marginally increased to 7%. Since the CD47 expression level on MDA-MB-231 cells is relatively high (Supplementary Fig. 3) and we were not able to further improve the IgA-mediated lysis by increasing the antigen expression level, we combined IgA with CD47 blockade. Lysis was enhanced from 3×10^5 HER2 molecules per cell onwards and it reached similar levels as that of IgG-mediated lysis at 5.7×10^5 molecules per cell. In line with our earlier observations, CD47 blockade did not enhance IgG-mediated lysis. Overall, these data are consistent with the results earlier, indicating that IgA-mediated lysis by PMNs is more restricted at lower antigen expression levels, which could potentially be related to the CD47 expression on the tumor cells.

A higher antigen level threshold for IgA is also observed with EpCAM.

We next investigated whether these findings would hold true for other antigens. Using the same Tet-on system, we transduced EpCAM into HeLa cells. A similar procedure was used to select low and high expressing clones (HeLa-EpCAM-Low and HeLa-EpCAM-High). Dox concentrations ranging from 0 to 1 ug/mL induced EpCAM expression on both clones. EpCAM expression in HeLa-EpCAM-low was induced from 5×10^3 up to 1.5×10^5 molecules per cell; whereas, the expression in HeLa-EpCAM-high ranged from 2×10^5 to 8×10^5 EpCAM molecules (Fig. 3). Subsequently, we conducted ADCC assays against these induced cells using the IgG heING1 antibody (anti-EpCAM) or its IgA counterpart.

Our findings have revealed a potential antigen level threshold, which appears to apply to both IgG and IgA antibodies. However, IgA antibodies seems to require higher expression levels to effectively induce ADCC. IgG-mediatedlysis remained low with only 5% lysis observed at very low expression levels. A gradual increase in lysis was only observed when the antigen expression level reached approximately 5.8×10^3 EpCAM molecules per cell, ultimately reaching a plateau at 10–15% lysis at 6×10^4 molecules per cell, which remained constant at higher expression levels. In contrast, IgA-mediated killing remained ineffective at lower antigen levels, only slowly
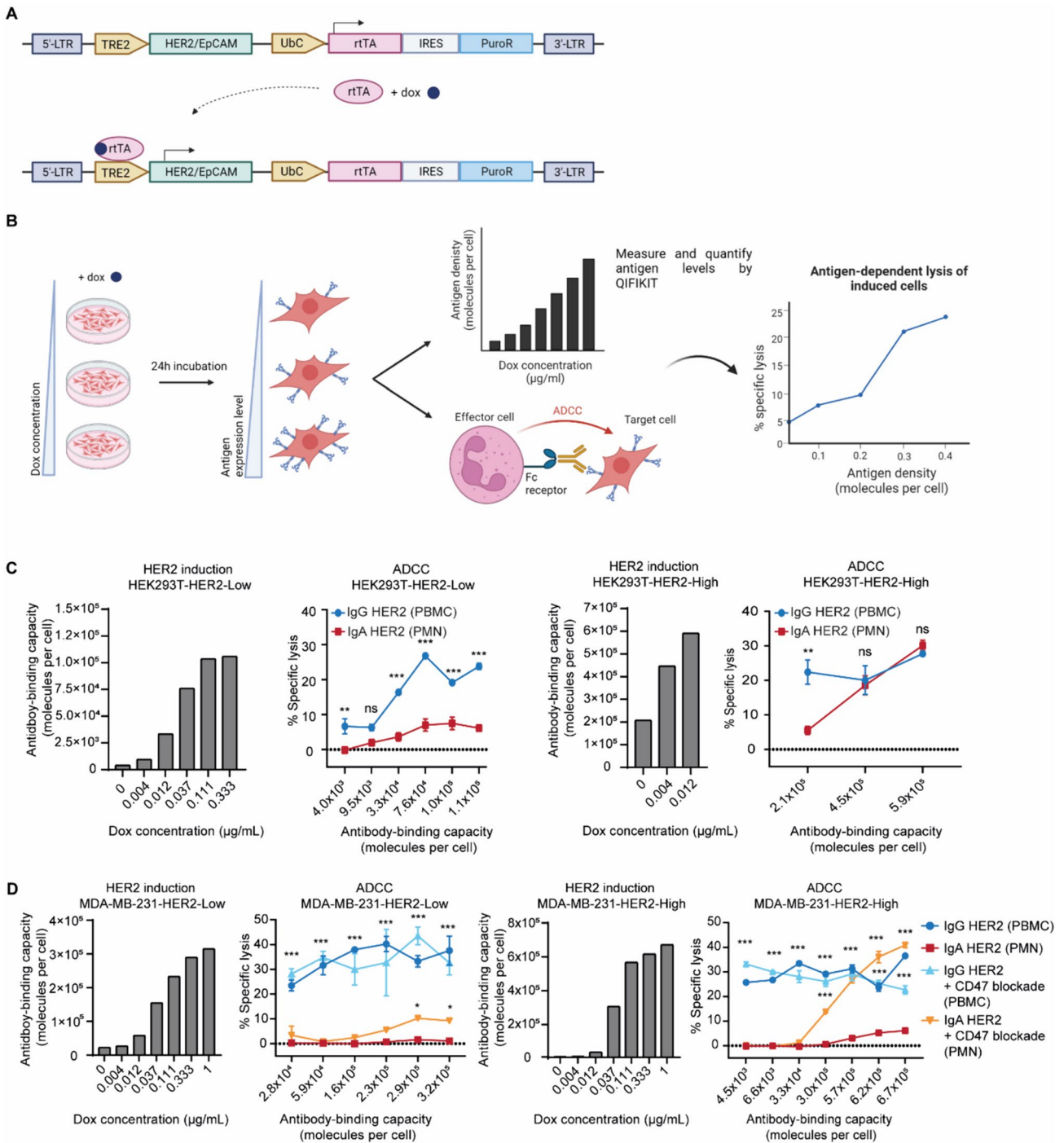
increased when the expression level exceeded 2.4×10^5 molecules per cell. Interestingly, at around 4.9×10^5 molecules per cell, IgA-mediated lysis reached levels comparable to IgG-mediated killing. As antigen expression levels increased, IgA-mediated lysis outperformed IgG-mediated lysis. Despite HeLa cells expressing CD47, combining IgA with CD47 blockade did not enhance specific lysis, in contrast to IgG combined with CD47 blockade, which did improve lysis at higher antigen levels (Supplementary

Fig. 3, Fig. 3). Further analysis indicated that the enhancement was not related to the IgG mAb (data not shown). It appears that the ADCC capacity was already elevated in the antibody negative control, suggesting an interaction between the PBMCs and the elevated expression levels. This observation, specific to this cell line, implies that intrinsic anti-tumor signals may have activated the NK cells or monocytes. Since this effect was only observed in this particular cell line, we did not investigate it further.

◄**Fig. 2** ADCC capacity related to dox-inducible HER2 expression in HEK293T-HER2 and MDA-MB-231-HER2 cells. **A** Schematic representation of the Tet-On inducible system. A ubiquitin C promoter (UbC) controls the expression of rtTA (reverse tetracycline transactivator) and puromycin resistance (PuroR). In the presence of doxycycline (dox), rtTA undergoes conformational changes and binds to TRE2 (tetracycline response element 2), leading to the translation of the target gene. **B** Overview of the experimental setup: Cells are cultured with varying dox concentrations for 24-h, resulting in titrated levels of antigen expression. These cells are subsequently tested in ADCC experiments, with concurrent quantification of antigen levels using QIFIKIT. Antigen expression levels are correlated to antibody-mediated killing. The graphs presented here are illustrative and do not represent actual data. **C** IgG and IgA-mediated ADCC assays against two HEK293T-HER2 clones with low and high HER2 expression levels. The ADCC assays for both clones were performed using effector cells from a single donor and repeated across three different donors (biological triplicates). One representative assay of each clone is shown. **D** ADCC assay against MDA-MB-231-HER2 (low and high expression) cells, using IgG HER2, IgA HER2, and IgA HER2 in combination with CD47 blockade. Effector cells were isolated from a healthy donor. For MDA-MB-231-HER2 with low expression, assays were performed in technical triplicates and independently repeated with 2 donors; while, those with high expression were done in technical triplicates and independently repeated with 3 donors. A representative graph for each clone is shown. In all ADCC assays, dox in concentration indicated in the graphs were used to induce HER2 expression. HER2 levels were quantified with 10 µg/mL HER2 antibody in a QIFIKIT assay. Lysis was assessed in a ^{51}Cr release assay using PBMCs (E:T 100:1) for IgG-mediated and PMNs (40:1) for IgA-mediated cytotoxicity. Cytotoxicity was evaluated with 10 µg/mL antibody, with optional CD47 blocking by 10 µg/mL SIRPα fusion protein. The mean ± SEM of specific lysis is shown. Statistical significance as compared to IgA HER2: ns > 0.05, *$p < 0.05$, **$p < 0.01$, ***$p < 0.001$, determined by two-way ANOVA followed by Tukey's multiple comparisons test. Illustrations were created using Biorender

Expression level dependency of IgA in a preclinical mouse model.

Subsequently, we aimed to investigate whether the antigen expression level dependency observed in vitro could also be observed in a preclinical mouse model. To explore this, we used modified A431 cells: A431-luc2 cells and A431-luc2-HER2 cells, with the latter having higher HER2 expression levels, similar to that of SK-BR-3 cells (Fig. 4A). In a ^{51}Cr release ADCC assay, the HER2 expression on A431-luc2 cells was too low to be susceptible to IgA HER2-mediated lysis; whereas, IgG HER2 induced specific lysis of 20% (Fig. 4B). The addition of CD47 blockade to IgA HER2 merely improved the lysis of A431-luc2, failing to match the levels achieved by IgG-mediated killing. In contrast, A431-luc2-HER2 could be effectively lysed by both IgG and IgA antibodies. In addition, CD47 blockade further enhanced the specific lysis of A431-luc2-HER2 cells, resulting in a 70% lysis rate.

To address the antigen level dependency in a mouse model, we injected 1×10^5 A431-luc2 cells intraperitoneally into SCID mice. Mice received treatment starting from day 5, with either 2 mg/kg IgG HER2 once a week or 2 mg/kg IgA HER2 three times a week. PBS was administered as solvent control in the control treatment group. Growth was monitored twice a week using bioluminescence imaging of the luc2-positive cells (Fig. 4C). IgG treatment efficiently impaired tumor growth; while, IgA treatment failed to decrease the tumor burden and showed a similar outgrowth as the solvent control. These outcomes are likely due to the low HER2 expression on the tumor cells, and in line with our previous observations in vitro. Remarkably, despite the modest improvement observed with CD47 blockade in vitro, treatment with 2 mg/kg IgA HER2 three times a week and an additional 30 mg/kg SIRPα fusion protein on days 5, 14, 24, and 33 impeded tumor growth to a similar extent as IgG therapy. Importantly, in an earlier mouse experiment that included different tumor cells, the use of CD47 blockade as a single agent did not impact tumor growth (**Data not shown**). Subsequently, in a similar mouse experiment using A431-luc2-HER2 cells, with high HER2 expression levels, both IgG HER2 and IgA HER2 therapies reduced the tumor burden, consistent with our in vitro assay results (Fig. 4D). Collectively, our results indicate that both the expression level and the presence of CD47 on tumor cells play an important role in IgA-mediated cytotoxicity.

IgA selectively targets lymphoma cells without affecting endogenous B cells

We considered that the absence of IgA-mediated cytotoxicity in cells expressing lower antigen levels may present an important clinical advantage. Healthy cells often express similar antigens as those commonly targeted on tumors, albeit usually at significantly lower expression levels, as seen with rituximab (IgG CD20). To evaluate the antigen threshold hypothesis, we used the murine B cell lymphoma cell line BCL-1, which expresses high levels of mCD20 (Fig. 5A). Utilizing a tumor mouse model with BCL-1 cells allowed us to test our antibodies in an environment, where mCD20 is expressed on both endogenous B cells and tumor cells. Notably, the mCD20 expression level on BCL-1 is significantly higher than that on the endogenous cells (Fig. 5A). This observation suggests that IgA therapy could serve as a potential strategy to avoid on-target, off-tumor side effects. To test this hypothesis, we administered a single dose of either PBS, murine afucosylated IgG2a mCD20 or human IgA-Alb8 mCD20 to CD89 Tg Balb/c mice. Both isotypes consist of the same mCD20 clone, ensuring comparable target specificity. To compare the most effective IgG isotype with IgA, we included the afucosylated murine IgG2a variant, which is adapted to enhance ADCC. Additionally, we used the IgA-Alb8 variant, which, while not enhancing ADCC, features an improved half-life due to albumin-binding modifications that address the typically short half-life of
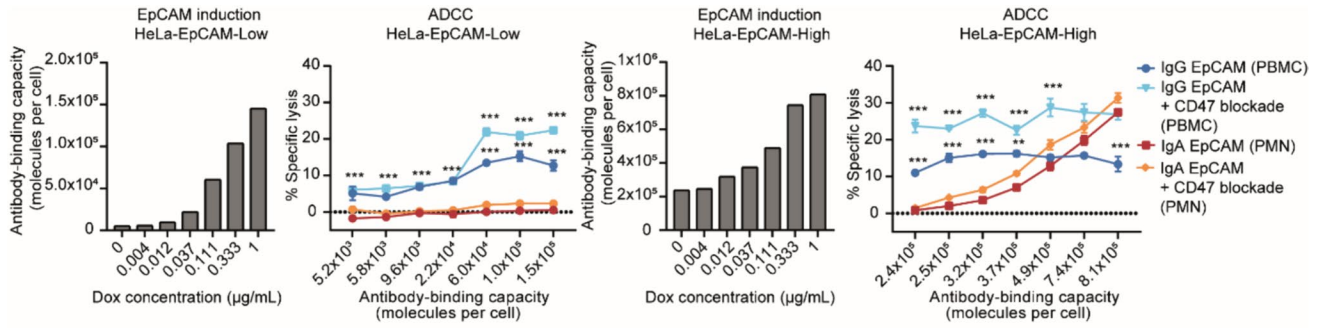
Fig. 3 Antibody-mediated ADCC capacity on dox-inducible HeLa-EpCAM cells. EpCAM expression was induced using doxycycline concentrations ranging from 0 to 1 μg/mL and quantified through QIFIKIT with a primary EpCAM antibody concentration of 10 μg/mL. ADCC assays utilized PBMCs (E:T 100:1) for IgG and PMNs (40:1) for IgA, with antibody concentrations of 10 μg/mL. CD47 was blocked using 10 μg/mL SIRPα fusion protein. Effector cells were freshly isolated from a healthy donor. Experiment was repeated in at least three different clones. Significance is shown as compared to IgA-mediated lysis. Specific lysis is shown as mean ± SEM. ns > 0.05, ***$p < 0.001$, by two-way ANOVA followed by Tukey's multiple comparisons test

IgA. Subsequently, B cell depletion was evaluated using flow cytometry (Fig. 5B). Blood, spleen, liver, bone marrow and lymph nodes were collected at multiple time points up to day 7. Intriguingly, injecting IgG antibody led to rapid depletion of B cells, with a noticeable effect as early as day 1, evident in both blood and the organs. Within just 2 days, virtually all endogenous B cells in the blood were depleted. Only B cells in the bone marrow remained largely unaffected. In contrast, IgA treatment did not deplete B cells and showed no significant impact throughout the 7-day period.

Following this, a murine lymphoma mouse model was established using BCL-1-luc2 cells to test the anti-tumoral effects of the mCD20 antibodies. Mice were intravenously injected with 5×10^5 BCL-1-luc2 cells, whereafter treatment with either PBS, murine afucosylated IgG2a mCD20 or human IgA-Alb8 mCD20started at day 3. Subsequently, the tumor growth was monitored using BLI measurements performed twice a week (Fig. 5C). Interestingly, while IgA treatment did not deplete the endogenous B cells, it proved to be highly effective in suppressing tumor growth in BCL-1 tumor-bearing mice (Fig. 5D, E). In comparison, IgG, which efficiently depleted endogenous B cells, failed to inhibit tumor growth in these mice. Our findings highlight the effectiveness of IgA in suppressing tumor growth without affecting healthy B cells, a significant advantage over IgG which depleted healthy B cells and failed in tumor cell targeting.

Discussion

Our study demonstrated that IgA antibodies require a higher threshold of antigen expression compared to IgG to effectively induce ADCC. Using a panel of breast cancer cells with varying HER2 expression levels, we observed an increase in the ADCC capacity elicited by both IgG and IgA antibodies as the HER2 expression level increased. This was further supported using dox-inducible cell line-based experiments. Interestingly, the onset of effective tumor lysis occurred at lower expression levels for IgG when compared to IgA antibodies. Our findings are in line with previous literature, in which studies reported that low expression levels of CD20 and EGFR were sufficient to induce ADCC by NK, monocytes or PBMC effector cells using IgG mAbs [25–27]. Moreover, previous research with IgA antibodies reported that specific lysis of tumor target cells occurred only when antigen expression was high [26, 28].

Using our dox-inducible cell lines we have identified a threshold of approximately $2–3 \times 10^5$ HER2 or EpCAM molecules per cell to instigate IgA-mediated ADCC by neutrophils. In contrast, the IgG threshold appears to be approximately 10 times lower. Moreover, in our A431 xenograft mouse model, we observed an anti-tumoral response with IgG therapy but not with IgA therapy against the low HER2-expressing A431-luc2 tumor; while, both IgG and IgA therapies were effective against the high HER2-expressing A431-luc2-HER2 tumor and suppressed tumor growth. The difference in antigen sensitivity between IgG and IgA may be explained by the distinct mechanisms of action of their respective effector immune cells. NK cells, the primary effector cells in PBMC-mediated ADCC, eliminate tumor cells by releasing cytotoxic granules filled with perforin and granzymes [54]. In contrast, neutrophils employ trogocytosis, a process in which small bites of the tumor cell membrane are engulfed, leading to a specific type of necrotic death known as trogoptosis [55]. Therefore, the observed differences might not be inherent to the antibody isotype, but rather to the effector cells engaged. This distinction could be strategically used in the clinic, allowing us to use IgA against ubiquitously expressed targets while
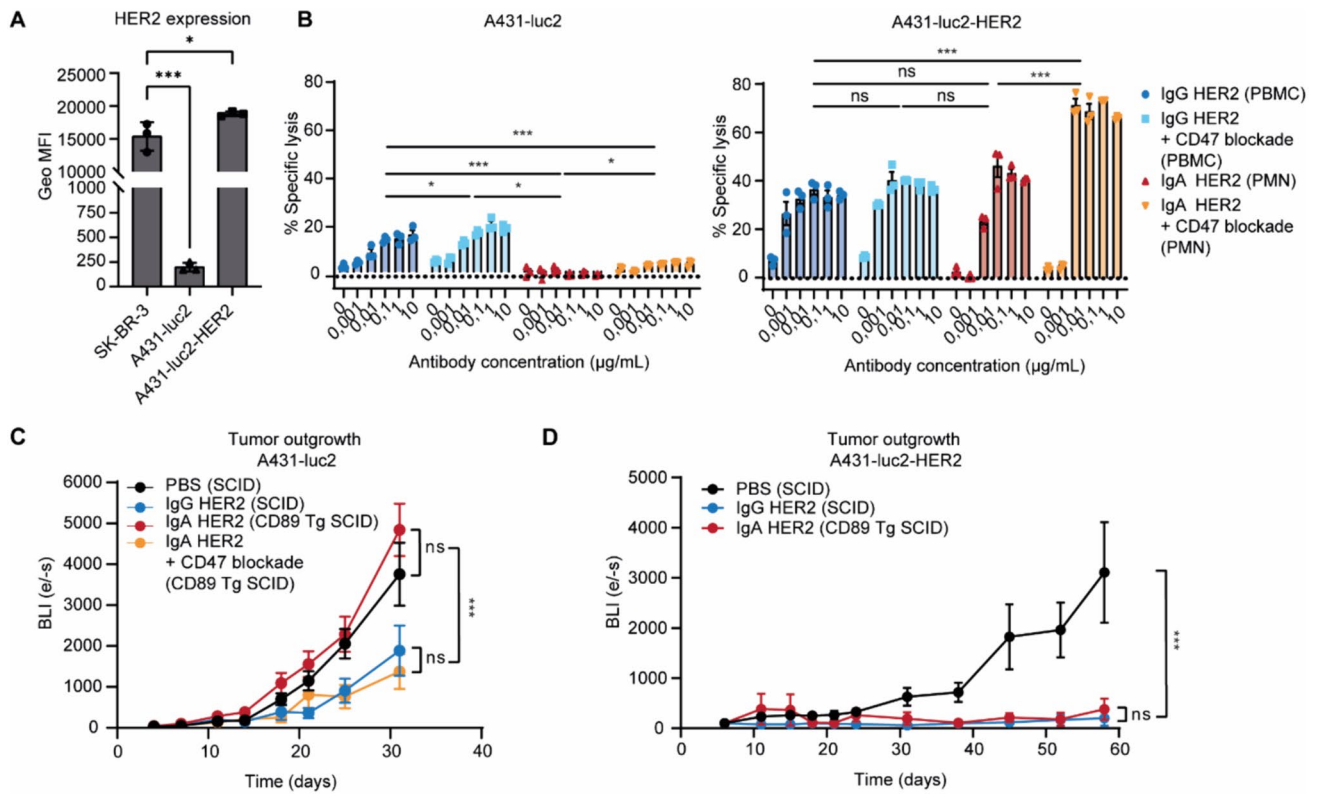
Fig. 4 Anti-tumoral effect of IgG HER2 and IgA HER2 in A431-luc2 tumor-bearing mice. **A** HER2 expression levels of A431-luc2 and A431-luc2-HER2 in comparison with SK-BR-3, measured via flow cytometry. The mean ± SD of geometric MFI is presented. *p < 0.05, ***p < 0.001, determined using one-way ANOVA with Bonferroni's multiple comparisons test. **B** IgG HER2 and IgA HER2 lysis against A431-luc2 and A431-luc2-HER2 cells were evaluated using PBMCs (E:T 100:1) for IgG and PMNs (40:1) for IgA. Antibody concentrations ranged from 0 to 10 µg/mL. CD47 was pre-blocked with 10 µg/mL SIRPα fusion protein. The assay was performed in technical triplicates using effector cells from a single healthy donor and was repeated three times with independent donors (biological triplicates).Individual values and the mean ± SEM of specific lysis from one representative experiment are presented. ns > 0.05, *p < 0.05 ***p < 0.001, as determined by two-way ANOVA followed by Tuk-

ey's multiple comparisons test. **C** Bioluminescence imaging (BLI) measurements depicting the tumor growth of A431-luc2 tumor in (CD89 Tg) SCID mice. Detailed treatment regimen is outlined in the methods section. Tumor sizes are presented as mean ± SEM. *p < 0.05, **p < 0.01, ***p < 0.001, as determined by two-way ANOVA followed by Tukey's multiple comparisons test. **D** Tumor outgrowth of A431-luc2-HER2 tumors in (CD89 Tg) SCID mice assessed through BLI. The detailed treatment regimen is provided in the methods section. BLI measurements are shown as BLI signal intensity, measured in photons per second (e/-s), and are displayed as the mean ± SEM. Statistical significance (ns > 0.05, ***p < 0.001) was determined using two-way ANOVA followed by Tukey's multiple comparisons test. For both in vivo experiments, CD89 Tg SCID mice were used in the groups receiving IgA; while, wild-type SCID mice were used for the other groups

minimizing damage to healthy tissues, which usually express lower antigen levels.

For example, healthy breast tissue expresses approximately 2×10^4 HER2 molecules per cell [56, 57]. At this level of antigen expression, IgG antibodies have been shown to induce cytotoxicity as demonstrated with HEK293T-HER2, MDA-MB-231-HER2 and HeLa-EpCAM cells. Modest HER2 expression is also observed in other healthy tissues, including the gastrointestinal tract, respiratory and reproductive systems, as well as the heart and skeletal muscles. According to data from the Human Protein Atlas, these tissues express a medium level of HER2 expression, similar to that in breast tissue [58], which may also be susceptible to targeting by IgG HER2 antibodies. This is clinically

relevant, especially considering that trastuzumab-induced cardiotoxicity has been well-documented when the mAb is used in combination with specific chemotherapeutic drugs [15–17, 59]. Next-generation therapies like the antibody–drug conjugate T-DXd have shown remarkable efficacy in breast cancer, leading to its accelerated approval for HER2-positive metastatic cases. Interestingly, T-DXd has significantly enhanced survival rates for patients with HER2-low tumors, addressing a previously difficult to treat population. Nevertheless, T-DXd treatment is associated with drug-related interstitial lung disease or pneumonitis, which demands close monitoring, potential dosage modification, or glucocorticoid intervention [60]. These challenges highlight the continued need for safer and more effective
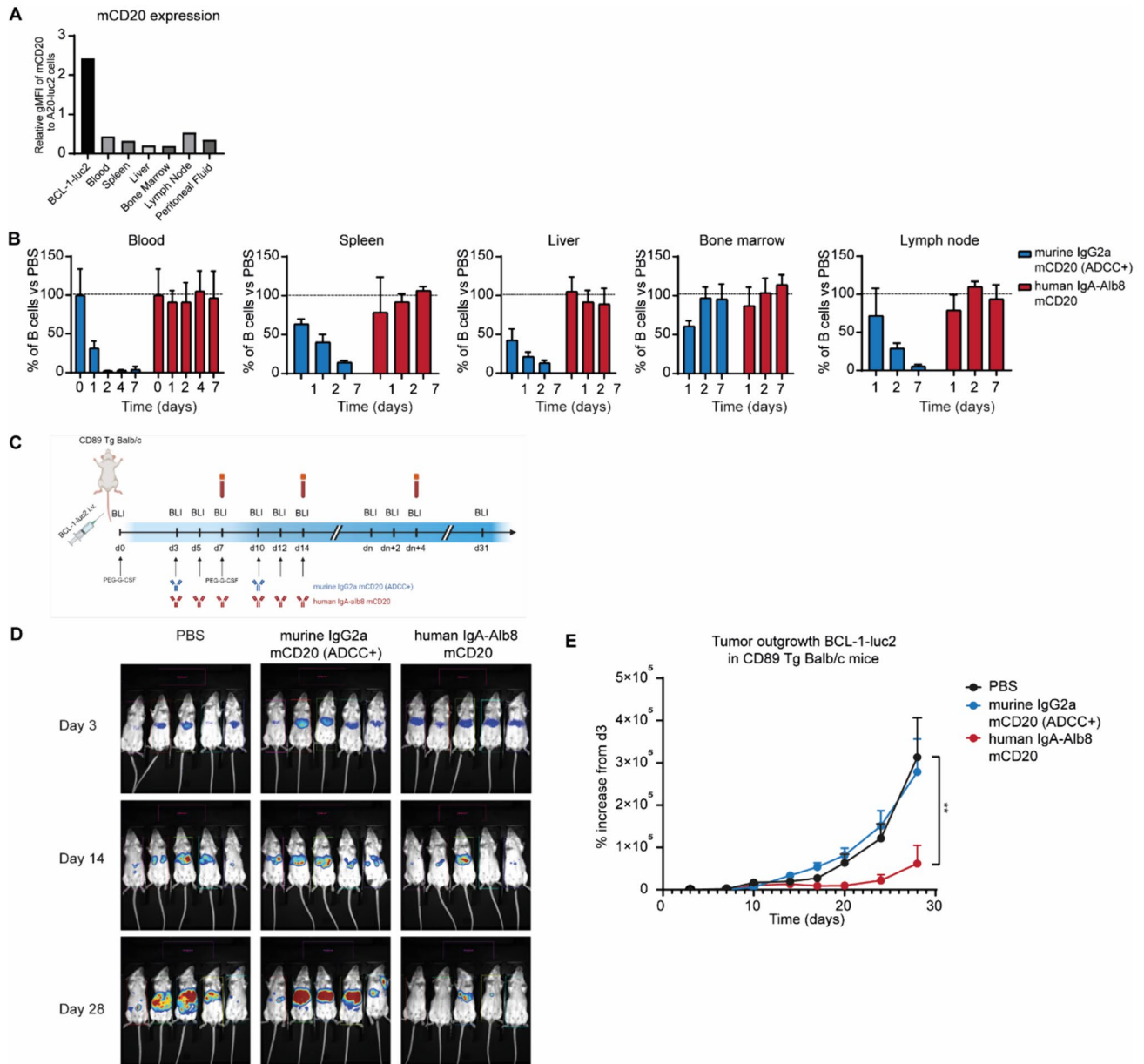
Fig. 5 IgA-mediated selective targeting of lymphoma cells while preserving endogenous B cells **A** The mCD20 expression level of BCL-1-luc2 cells was compared to endogenous B cells in Balb/c mice, measured via flow cytometry. **B** The depletion of endogenous B cells was monitored following a single dose of either PBS, 5 mg/kg murine afucosylated IgG2a mCD20, or 5 mg/kg human IgA-Alb8 mCD20 in CD89 Tg Balb/c mice for up to 7 days. The percentage of B cells, compared to the PBS vehicle control, was measured in blood, spleen, liver, bone marrow, and lymph nodes, and the results are presented as mean ± SD. **C** A schematic overview of the syngeneic BCL-1 lymphoma model in CD89 Tg Balb/c mice. In brief, a total of 5×10^5 BCL-1-luc2 cells and a dose of PEG-G-CSF were injected on day 0, followed by another PEG-G-CSF dose on day 7. Treatment with PBS, 6 mg/kg murine afucosylated IgG2a mCD20, or 6 mg/kg human IgA-Alb8 mCD20 began on day 3. IgA was administered on days 3, 5, 7, 10, 12, and 14; while, IgG was given on days 3 and 10. The dosage frequency differs because of the isotype's different half-lives. This dosing regimen is optimized to maintain similar serum titers. Tumor growth was monitored by bioluminescence imaging twice a week. **D** Representative BLI images of the different treatment groups on day 3, 14 and 28. **E** BCL-1 tumor outgrowth is depicted as a percentage increase in BLI signal from day 3. The percentages are presented as mean ± SEM. **p < 0.01, determined by two-way ANOVA followed by Tukey's multiple comparisons test

treatments. Moreover, EpCAM, being a highly expressed antigen in adenocarcinomas, is a desirable target. However, a vast majority of healthy tissues also express EpCAM, particularly in the gastrointestinal tract [61]. High-affinity EpCAM-targeting antibodies, such as ING-1 and 3622W94, have shown dose-limiting side effects, including pancreatitis

[62]. Similarly, Solitomab, a bispecific T-cell engager targeting EpCAM, led to dose-limiting side effects in 95% of participating patients in a phase 1 study [63]. Another example of on-target, off-tumor side effects is the hypogammaglobulinemia observed in pediatric non-Hodgkin's lymphoma patients receiving rituximab. These children experience long-term B cell depletion, impairing memory B cell development, which often leads to an increased susceptibility to infections [19, 20]. This makes achieving a therapeutic effect more difficult, as reducing the antibody's affinity can decrease toxicity but often results in limited therapeutic efficacy. Due to the significantly higher antigen expression threshold of IgA compared to IgG, healthy tissues are likely to be unaffected by IgA-mediated targeting. This hypothesis is supported by our B cell depletion assay and BCL-1 lymphoma mouse model, where we observed that IgG depleted endogenous murine B cells, except those derived from the bone marrow, while IgA did not deplete any of the endogenous B cells. B cells in the bone marrow compartment could have been spared by IgG due to higher expression of inhibitory FcγRs in the bone marrow niche [64]. Moreover, IgA likely did not deplete bone marrow-derived B cells due to low mCD20 expression and the lower expression levels of FcαRI (CD89) on bone marrow-resident granulocytes [65, 66]. Remarkably, IgA, while sparing healthy B cells, demonstrated a superior anti-tumor response against the BCL-1 tumor, which expresses mCD20 at a level three times higher than endogenous B cells. To our surprise, IgG did not show any anti-tumor response at all. While afucosylated IgG antibodies show enhanced ADCC capacity in patients, this may not translate to mouse models due to differences in Fcγ receptor interactions [53]. Although the IgG results in the BCL-1 model did not meet our expectations, we think the overall message remains clear: IgA did not affect healthy circulating B cells but demonstrated a significant anti-tumor response in mice.

Our findings support the idea that the difference in response between IgG and IgA is partly due to the overexpression of CD47 on tumor cells, which suppresses IgA-mediated neutrophil activation. In some experiments, inhibiting CD47 increased cytotoxicity to levels comparable to IgG-mediated lysis. However, this is not consistently observed across all tested cell lines, and the enhancement is often most noticeable when combined with medium to high target antigen expression levels. In some instances, IgG was able to effectively induce PBMC-mediated lysis at lower expression levels; whereas, the addition of CD47 blockade to IgA did not result in lysis rates comparable to those achieved by IgG. Moreover, we observed an increase in IgG-mediated lysis upon CD47 inhibition in HeLa-EpCAM cells, which was observed in the absence of antibody. This suggests the presence of an alternate pro-phagocytic signal, but since this was only observed in one cell line, we did not investigate further. Additionally, it is important to consider the level of CD47 expression, as it varies among different tumors. Moreover, it is possible that a high antigen expression level is less influenced by checkpoint molecules, such as the CD47/SIRPα axis, as we observed that the fold change enhancement is less pronounced at higher target expression levels. Consequently, the ratio of antigen expression to CD47 expression should be further explored. In summary, IgA cytotoxicity is more dependent on antigen expression level compared to IgG, and myeloid checkpoints like the CD47/SIRPα axis may contribute to this threshold of antigen expression. Therefore, IgA therapy would not be recommended for cases with significant antigen loss caused by mechanisms such as antigen shaving post-IgG therapy [67]. However, when antigen expression levels are marginal, the addition of CD47 blockade to IgA therapy could be considered to enhance its efficacy.

Several strategies have been proposed to mitigate on-target, off-tumor side effects. For example, using an antibody with a pH-sensitive linker, allowing it to bind specifically to tumor antigens in the acidic tumor microenvironment [68]. In another approach, anti-CD47 antibodies were pre-bound to vesicles containing a specific number of CD47 molecules. The antibody is only released from the vesicle at sites where CD47 expression levels are high enough to compete with the bound CD47 molecules on the vesicle, which are typically within the tumor [22]. While promising, this approach is intricate and involves a lengthy vesicle manufacturing process. In contrast, IgA antibodies provide a more straightforward solution. The IgA therapeutic has been extensively characterized and can be readily tailored to target various antigens. Moreover, the engineered IgA3.0 antibody has been optimized for production and purification, making it ready for clinical translation and therapeutic use [52].

In conclusion, our study highlights the importance of antigen expression thresholds in targeted immunotherapy, with IgA requiring a higher threshold compared to IgG. Therefore, IgA holds the potential to reduce on-target off-tumor side effects, which are sometimes associated with IgG therapy. These advancements could potentially improve current immunotherapeutic approaches, fostering further development in the field.

Author contributions Conceptualization contributed by CC, GT, JHWL. Methodology contributed by CC, VGM, GT. Formal Analysis contributed by CC, NCC. Investigation contributed by CC, NCC, JHMJ, MN, EMP, JG. Resources contributed by VGM, MP.

Declarations

Conflict of interest The authors declare no competing interests.

Consent of publication The publication has been approved by all co-authors.

Ethical approval This study involves human participants and was approved by UMC Utrecht 07–125. Participants gave informed consent to participate in the study before taking part. All animal experiments followed international guidelines and were approved by the national Central Authority for Scientific Procedures on Animals (CCD) and the local experimental animal welfare organization (AVD115002016410).

References

1. Zeller T, Lutz S, Münnich IA, Windisch R, Hilger P, Herold T, Tahiri N, Banck JC, Weigert O, Moosmann A et al (2022) Dual checkpoint blockade of CD47 and LILRB1 enhances CD20 antibody-dependent phagocytosis of lymphoma cells by macrophages. Front Immunol. https://doi.org/10.3389/fimmu.2022.929339

2. Fan X, Krieg S, Kuo CJ, Wiegand SJ, Rabinovitch M, Druzin ML, Brenner RM, Giudice LC, Nayak NR (2008) VEGF blockade inhibits angiogenesis and reepithelialization of endometrium. FASEB J. https://doi.org/10.1096/fj.08-111401

3. de Taeye SW, Bentlage AEH, Mebius MM, Meesters JI, Lissenberg-Thunnissen S, Falck D, Sénard T, Salehi N, Wuhrer M, Schuurman J et al (2020) FcγR binding and ADCC activity of human IgG allotypes. Front Immunol. https://doi.org/10.3389/fimmu.2020.00740

4. Zinn S, Vazquez-Lombardi R, Zimmermann C, Sapra P, Jermutus L, Christ D (2023) Advances in antibody-based therapy in oncology. Nat Cancer 4:165–180

5. Goydel RS, Rader C (2021) Antibody-based cancer therapy. Oncogene 40:3655–3664

6. Lu LL, Suscovich TJ, Fortune SM, Alter G (2018) Beyond binding: antibody effector functions in infectious diseases. Nat Rev Immunol 18:46

7. Wang W, Erbe AK, Hank JA, Morris ZS, Sondel PM (2015) NK cell-mediated antibody-dependent cellular cytotoxicity in cancer immunotherapy. Front Immunol 6:368

8. Getahun A, Cambier JC (2015) Of ITIMs, ITAMs, and ITAMis: revisiting immunoglobulin Fc receptor signaling. Immunol Rev 268:66

9. Wang Y, Jönsson F (1958) Expression, role, and regulation of neutrophil Fcγ receptors. Front Immunol 2019:10

10. Ventola CL (2017) Cancer immunotherapy, part 2: efficacy, safety, and other clinical considerations. Pharm Ther 42(7):452

11. Tabrizi MA, Roskos LK (2007) Preclinical and clinical safety of monoclonal antibodies. Drug Discov Today 12(13–14):540–7

12. Krishna A, Sathya M, Mukesh S, Athiyamaan MS, Banerjee S, Sunny J, Srinivas C, Lobo D, Makkapatti BS, Jawahar V (2023) Efficacy and safety of EGFR inhibitor gefitinib in recurrent or metastatic cervical cancer: a preliminary report. Med Oncol. https://doi.org/10.1007/s12032-023-02070-1

13. Petrelli F, Ardito R, Ghidini A, Zaniboni A, Ghidini M, Barni S, Tomasello G (2018) Different toxicity of cetuximab and panitumumab in metastatic colorectal cancer treatment: a systematic review and meta-analysis. Oncology 94(4):191–9

14. Wollenberg A, Kroth J, Hauschild A, Dirschka T (2010) Cutaneous side effects of EGFR inhibitors appearance and management. Deutsche Medizinische Wochenschrift. https://doi.org/10.1055/s-0029-1244831

15. Mohan N, Jiang J, Dokmanovic M, Wu WJ (2018) Trastuzumab-mediated cardiotoxicity: current understanding, challenges, and frontiers. Antibody Ther 1(1):13–7

16. Grazette LP, Boecker W, Matsui T, Semigran M, Force TL, Hajjar RJ, Rosenzweig A (2004) Inhibition of ErbB2 causes mitochondrial dysfunction in cardiomyocytes: implications for herceptin-induced cardiomyopathy. J Am Coll Cardiol. https://doi.org/10.1016/j.jacc.2004.08.066

17. Nemeth BT, Varga ZV, Wu WJ, Pacher P (2017) Trastuzumab cardiotoxicity: from clinical trials to experimental studies. Br J Pharmacol 174(21):3727–48

18. Florido R, Smith KL, Cuomo KK, Russell SD (2017) Cardiotoxicity from human epidermal growth factor receptor-2 (HER2) targeted therapies. J Am Heart Assoc. https://doi.org/10.1161/JAHA.117.006915

19. Barmettler S, Ong MS, Farmer JR, Choi H, Walter J (2018) Association of immunoglobulin levels, infectious risk, and mortality with rituximab and hypogammaglobulinemia. JAMA Netw Open. https://doi.org/10.1001/jamanetworkopen.2018.4169

20. Labrosse R, Barmettler S, Derfalvi B, Blincoe A, Cros G, Lacombe-Barrios J, Barsalou J, Yang N, Alrumayyan N, Sinclair J et al (2021) Rituximab-induced hypogammaglobulinemia and infection risk in pediatric patients. J Allergy Clin Immunol. https://doi.org/10.1016/j.jaci.2021.03.041

21. Zhao Y, Baldin AV, Isayev O, Werner J, Zamyatnin AA, Bazhin AV (2021) Cancer vaccines: antigen selection strategy. Vaccines. https://doi.org/10.3390/vaccines9020085

22. Tang Z, Wang X, Tang M, Wu J, Zhang J, Liu X, Gao F, Fu Y, Tang P, Li C (2023) Overcoming the on-target toxicity in antibody-mediated therapies via an indirect active targeting strategy. Adv Sci. https://doi.org/10.1002/advs.202206912

23. Boland WK, Bebb G (2009) Nimotuzumab: a novel anti-EGFR monoclonal antibody that retains anti-EGFR activity while minimizing skin toxicity. Exp Opin Biol Ther 9(9):1199–206

24. Patel D, Guo X, Ng S, Melchior M, Balderes P, Burtrum D, Persaud K, Luna X, Ludwig DL, Kang X (2010) IgG Isotype, glycosylation, and EGFR expression determine the induction

of antibody-dependent cellular cytotoxicity in vitro by cetuximab. Hum Antibodies 19:89–99. https://doi.org/10.3233/HAB-2010-0232

25. Van Meerten T, Van Rijn RS, Hol S, Hagenbeek A, Ebeling SB (2006) Complement-induced cell death by rituximab depends on CD20 expression level and acts complementary to antibody-dependent cellular cytotoxicity. Clin Cancer Res. https://doi.org/10.1158/1078-0432.CCR-06-0066

26. Derer S, Bauer P, Lohse S, Scheel AH, Berger S, Kellner C, Peipp M, Valerius T (2012) Impact of epidermal growth factor receptor (EGFR) cell surface expression levels on effector mechanisms of EGFR antibodies. J Immunol. https://doi.org/10.4049/jimmunol.1202037

27. Kurai J, Chikumi H, Hashimoto K, Yamaguchi K, Yamasaki A, Sako T, Touge H, Makino H, Takata M, Miyata M et al (2007) Antibody-dependent cellular cytotoxicity mediated by cetuximab against lung cancer cell lines. Clin Cancer Res. https://doi.org/10.1158/1078-0432.CCR-06-1726

28. Brandsma AM, Bondza S, Evers M, Koutstaal R, Nederend M, Jansen JM, Rösner T, Valerius T, Leusen JH, Ten Broeke T (2019) Potent Fc receptor signaling by IgA leads to superior killing of cancer cells by neutrophils compared to IgG. Front Immunol 11(10):704. https://doi.org/10.3389/fimmu.2019.00704

29. Heemskerk N, Gruijs M, Temming AR, Heineke MH, Gout DY, Hellingman T, Tuk CW, Winter PJ, Lissenberg-Thunnissen S, Bentlage AE, De Donatis M (2021) Augmented antibody-based anticancer therapeutics boost neutrophil cytotoxicity. J Clin Invest. https://doi.org/10.1172/JCI134680

30. Brandsma AM, Ten Broeke T, Nederend M, Meulenbroek LA, van Tetering G, Meyer S, Jansen JM, Beltrán Buitrago MA, Nagelkerke SQ, Németh I, Ubink R (2015) Simultaneous targeting of FcγRs and FcαRI enhances tumor cell killing. Cancer Immunol Res 3(12):1316–24

31. Treffers LW, Ten Broeke T, Rösner T, Jansen JM, van Houdt M, Kahle S, Schornagel K, Verkuijlen PJ, Prins JM, Franke K, Kuijpers TW (2020) IgA-mediated killing of tumor cells by neutrophils is enhanced by CD47–SIRPα checkpoint inhibition. Cancer Immunol Res 8(1):120–30. https://doi.org/10.1158/2326-6066.CIR-19-0144

32. van Tetering G, Evers M, Chan C, Stip M, Leusen J (2020) Fc engineering strategies to advance IgA antibodies as therapeutic agents. Antibodies 9(4):70

33. Lohse S, Loew S, Kretschmer A, Jansen JH, Meyer S, Ten Broeke T, Rosner T, Dechant M, Derer S, Klausz K, Kellner C (2018) Effector mechanisms of IgA antibodies against CD20 include recruitment of myeloid cells for antibody-dependent cell-mediated cytotoxicity (ADCC), and complement dependent cytotoxicity (CDC). Br J Haematol 181(3):413–7

34. Lohse S, Meyer S, Meulenbroek LAPM, Jansen JHM, Nederend M, Kretschmer A, Klausz K, Möginger U, Derer S, Rösner T et al (2016) An Anti-EGFR IgA that displays improved pharmacokinetics and myeloid effector cell engagement in vivo. Cancer Res. https://doi.org/10.1158/0008-5472.CAN-15-1232

35. Stip MC, Evers M, Nederend M, Chan C, Reiding KR, Damen MJ, Heck AJR, Koustoulidou S, Ramakers R, Krijger GC et al (2023) IgA antibody immunotherapy targeting GD2 Is effective in pre-clinical neuroblastoma models. J Immunother Cancer 11:e006948. https://doi.org/10.1136/jitc-2023-006948

36. Breedveld A, Van Egmond M (2019) IgA and FcαRI: pathological roles and therapeutic opportunities. Front Immunol 10:553

37. Leusen JHW (2015) IgA as therapeutic antibody. Mol Immunol. https://doi.org/10.1016/j.molimm.2015.09.005

38. Peipp M, Van Bueren JJL, Schneider-Merck T, Bleeker WWK, Dechant M, Beyer T, Repp R, Van Berkel PHC, Vink T, Van De Winkel JGJ et al (2008) Antibody fucosylation differentially impacts cytotoxicity mediated by NK and PMN effector cells. Blood. https://doi.org/10.1182/blood-2008-03-144600

39. Treffers LW, Van Houdt M, Bruggeman CW, Heineke MH, Zhao XW, Van Der Heijden J, Nagelkerke SQ, Verkuijlen PJJH, Geissler J, Lissenberg-Thunnissen S et al (2019) FcγRIIIb restricts antibody-dependent destruction of cancer cells by human neutrophils. Front Immunol. https://doi.org/10.3389/fimmu.2018.03124

40. van der Steen L, Tuk CW, Bakema JE, Kooij G, Reijerkerk A, Vidarsson G, Bouma G, Kraal G, de Vries HE, Beelen RHJ et al (2009) Immunoglobulin A: FcαRI interactions induce neutrophil migration through release of leukotriene B4. Gastroenterology. https://doi.org/10.1053/j.gastro.2009.06.047

41. Chan C, Lustig M, Baumann N, Valerius T, Van Tetering G, Leusen JH (2022) Targeting myeloid checkpoint molecules in combination with antibody therapy: a novel anti-cancer strategy with IgA antibodies? Front Immunol 5(13):932155

42. Logtenberg MEW, Jansen JHM, Raaben M, Toebes M, Franke K, Brandsma AM, Matlung HL, Fauster A, Gomez-Eerland R, Bakker NAM et al (2019) Glutaminyl cyclase is an enzymatic modifier of the CD47-SIRPα axis and a target for cancer immunotherapy. Nat Med. https://doi.org/10.1038/s41591-019-0356-z

43. Bouwstra R, van Meerten T, Bremer E (2022) CD47-SIRPα blocking-based immunotherapy: current and prospective therapeutic strategies. Clin Transl Med. https://doi.org/10.1002/ctm2.943

44. Willingham SB, Volkmer JP, Gentles AJ, Sahoo D, Dalerba P, Mitra SS, Wang J, Contreras-Trujillo H, Martin R, Cohen JD et al (2012) The CD47-signal regulatory protein alpha (SIRPa) interaction is a therapeutic target for human solid tumors. Proc Natl Acad Sci USA. https://doi.org/10.1073/pnas.1121623109

45. Baumann N, Arndt C, Petersen J, Lustig M, Rösner T, Klausz K, Kellner C, Bultmann M, Bastian L, Vogiatzi F et al (2022) Myeloid checkpoint blockade improves killing of T-acute lymphoblastic leukemia cells by an IgA2 variant of daratumumab. Front Immunol. https://doi.org/10.3389/fimmu.2022.949140

46. Evers M, Rosner T, Dunkel A, Marco Jansen H, Baumann N, ten Broeke T, Nederend M, Eichholz K, Klausz K, Reiding K et al (2021) The selection of variable regions affects effector mechanisms of IgA antibodies against CD20. Blood Adv. https://doi.org/10.1182/bloodadvances.2021004598

47. Chernyavska M, Hermans CKJC, Chan C, Baumann N, Rösner T, Leusen JHW, Valerius T, Verdurmen WPR (2022) Evaluation of immunotherapies improving macrophage anti-tumor response using a microfluidic model. Organs Chip 4:100019. https://doi.org/10.1016/j.ooc.2022.100019

48. Meyer S, Nederend M, Marco Jansen JH, Reiding KR, Jacobino SR, Meeldijk J, Bovenschen N, Wuhrer M, Valerius T, Ubink R et al (2016) Improved in vivo anti-tumor effects of IgA-Her2 antibodies through half-life extension and serum exposure enhancement by FcRn targeting. MAbs 8:87–98. https://doi.org/10.1080/19420862.2015.1106658

49. Brandsma, A.M.; ten Broeke, T.; Nederend, M.; Meulenbroek, L.A.P.M.; van Tetering, G.; Meyer, S.; Jansen, J.H.M.; Beltran Buitrago, M.A.; Nagelkerke, S.Q.; Nemeth, I.; et al. Simultaneous Targeting of Fc Rs and Fc RI Enhances Tumor Cell Killing. *Cancer Immunol Res* **2015**, https://doi.org/10.1158/2326-6066.CIR-15-0099-T.

50. Van Egmond M, Van Vuuren AJH, Morion HC, Van Spriel AB, Shen L, Hofhuis FMA, Saito T, Mayadas TN, Verbeek JS, Van De Winkel JGJ (1999) Human immunoglobulin a receptor (FcαRI, CD89) function in transgenic mice requires both FCR γ chain and CR3 (CD11b/CD18). Blood 93:4387–4394. https://doi.org/10.1182/blood.v93.12.4387.412k08_4387_4394

51. Stip MC, Jansen JHM, Nederend M, Tsioumpekou M, Evers M, Olofsen PA, Meyer-Wentrup F, Leusen JHW (2023) Characterization of human Fc alpha receptor transgenic mice: comparison of cd89 expression and antibody-dependent tumor killing between

mouse strains. Cancer Immunol Immunother 72:3063. https://doi.org/10.1007/S00262-023-03478-4

52. Evers M, Stip M, Keller K, Willemen H, Nederend M, Jansen M, Chan C, Budding K, Nierkens S, Valerius T et al (2021) Anti-GD2 IgA kills tumors by neutrophils without antibody-associated pain in the preclinical treatment of high-risk neuroblastoma. J Immunother Cancer 9:e003163. https://doi.org/10.1136/jitc-2021-003163

53. Silence K, Dreier T, Moshir M, Ulrichts P, Gabriels SME, Saunders M, Wajant H, Brouckaert P, Huyghe L, Van Hauwermeiren T et al (2014) ARGX-110, a highly potent antibody targeting CD70, eliminates tumors via both enhanced ADCC and immune checkpoint blockade. MAbs. https://doi.org/10.4161/mabs.27398

54. Trapani JA, Smyth MJ (2002) Functional significance of the perforin/granzyme cell death pathway. Nat Rev Immunol 2:735

55. Matlung HL, Babes L, Zhao XW, van Houdt M, Treffers LW, van Rees DJ, Franke K, Schornagel K, Verkuijlen P, Janssen H et al (2018) Neutrophils kill antibody-opsonized cancer cells by trogoptosis. Cell Rep 23:3946-3959.e6. https://doi.org/10.1016/j.celrep.2018.05.082

56. Ross JS, Fletcher JA, Bloom KJ, Linette GP, Stec J, Clark E, Ayers M, Symmans WF, Pusztai L, Hortobagyi GN (2003) HER-2/Neu testing in breast cancer. Pathol Patterns Rev 120(suppl1):S53-71

57. Press MF, Cordon-Cardo C, Slamon DJ (1990) Expression of the HER-2/Neu proto-oncogene in normal human adult and fetal tissues. Oncogene 5(7):953–62

58. Uhlén M, Fagerberg L, Hallström BM, Lindskog C, Oksvold P, Mardinoglu A, Sivertsson Å, Kampf C, Sjöstedt E, Asplund A et al (1979) Tissue-based map of the human proteome. Science 2015:347. https://doi.org/10.1126/science.1260419

59. Sawaya H, Sebag IA, Plana JC, Januzzi JL, Ky B, Cohen V, Gosavi S, Carver JR, Wiegers SE, Martin RP et al (2011) early detection and prediction of cardiotoxicity in chemotherapy-treated patients. Am J Cardiol. https://doi.org/10.1016/j.amjcard.2011.01.006

60. Modi S, Jacot W, Yamashita T, Sohn J, Vidal M, Tokunaga E, Tsurutani J, Ueno NT, Prat A, Chae YS et al (2022) Trastuzumab deruxtecan in previously treated HER2-low advanced breast cancer. N E J Med. https://doi.org/10.1056/nejmoa2203690

61. Went PT, Lugli A, Meier S, Bundi M, Mirlacher M, Sauter G, Dirnhofer S (2004) Frequent EpCam protein expression in human carcinomas. Hum Pathol. https://doi.org/10.1016/j.humpath.2003.08.026

62. Münz M, Murr A, Kvesic M, Rau D, Mangold S, Pflanz S, Lumsden J, Volkland J, Fagerberg J, Riethmüller G et al (2010) Side-by-side analysis of five clinically tested anti-EpCAM monoclonal antibodies. Cancer Cell Int. https://doi.org/10.1186/1475-2867-10-44

63. Kebenko M, Goebeler ME, Wolf M, Hasenburg A, Seggewiss-Bernhardt R, Ritter B, Rautenberg B, Atanackovic D, Kratzer A, Rottman JB et al (2018) A multicenter phase 1 study of solitomab (MT110, AMG 110), a bispecific EpCAM/CD3 T-cell engager (BiTE®) antibody construct. Patients Refract Solid Tumors Oncoimmunology. https://doi.org/10.1080/2162402X.2018.1450710

64. Roghanian A, Hu G, Fraser C, Singh M, Foxall RB, Meyer MJ, Lees E, Huet H, Glennie MJ, Beers SA et al (2019) Cyclophosphamide enhances cancer antibody immunotherapy in the resistant bone marrow niche by modulating macrophage FcγR expression. Cancer Immunol Res 7:1876–1890. https://doi.org/10.1158/2326-6066.CIR-18-0835

65. Otten MA, Leusen JHW, Rudolph E, van der Linden JA, Beelen RHJ, van de Winkel JGJ, van Egmond M (2007) FcR γ-chain dependent signaling in immature neutrophils is mediated by FcαRI, but not by FcγRI. J Immunol 179:2918–2924. https://doi.org/10.4049/JIMMUNOL.179.5.2918

66. Kim M, Lu RJ, Benayoun BA (2022) Single-Cell RNa-Seq of primary bone marrow neutrophils from female and male adult mice. Sci Data 9(1):442. https://doi.org/10.1038/s41597-022-01544-7

67. Jones JD, Hamilton BJ, Rigby WFC (2012) Rituximab mediates loss of CD19 on B cells in the absence of cell death. Arth Rheum. https://doi.org/10.1002/art.34560

68. Zhao Y, Xie YQ, Van Herck S, Nassiri S, Gao M, Guo Y, Tang L (2021) Switchable immune modulator for tumor-specific activation of anticancer immunity. Sci Adv. https://doi.org/10.1126/sciadv.abg7291